ROBOMECH Journal

RESEARCH

Open Access

Interactive driving of electrostatic film actuator by proximity motion of human body

Akira Okuno[1*], Shunsuke Yoshimoto[1] and Akio Yamamoto[1]

Abstract

A built-in capacitive proximity sensing method for a charge-induction electrostatic film actuator is proposed. This actuator consists of two thin sheets that function as a stator and a slider. A stator is an insulating sheet with many strips of electrodes in it, whereas a slider is a dielectric sheet that has slight conductivity on its surface. By applying actuation voltage on stator electrodes, the slider that is placed on the stator is driven by electrostatic force. This research realized the simultaneous actuation and proximity sensing using the same electrodes by integrating a resonance-based capacitance measurement circuit into a driving circuit. The study investigated the impact of having a slider on sensing performance, confirming the feasibility of simultaneous sensing and driving. The implemented system achieved an interactive actuation that changed driving velocity according to the proximity distance of the human hand.

Keywords Electrostatic actuator, Proximity sensing, Capacitive sensing

Introduction

Charge-induction electrostatic actuators [1] are one type of macro-scale electrostatic actuators [2–6], which are realized on a centimeter-scale. In its typical configuration, the actuator consists of two films: a stator and a slider. The stator is a thin plastic sheet with many embedded parallel electrodes that are connected into multiple phases, such as 3-phase and 4-phase. The slider is also a thin plastic sheet but does not have any electrodes. Instead, it has slight conductivity on its surface to react to an electric field created by the stator electrodes. The slider is driven on the surface of the stator by applying a multi-phase voltage pattern to the stator's electrodes.

One characteristic feature of this actuator lies in its physical shape. While its thickness ranges from tens of micrometers to a few millimeters, it can be fabricated over a large area spanning from tens of centimeters up to a meter. Other unique features include its ability to be optically transparent [7], depending on the materials used, and its capability to have pictures printed on its surface [8].

Utilizing these unique features, several applications as human interfaces have been proposed for the actuator. One example is a vision-motion integrated display [9–11]. In this integrated display, a transparent stator of the actuator is integrated onto the surface of a visual display. A slider with a picture printed is placed on the display as a tangible object. A user can manually move the tangible slider to interact with or manipulate the visual information displayed beneath the stator. Alternately, the slider can be automatically moved by the electrostatic actuation to represent a response from the visual information. In such a way, users can experience bi-directional tangible interactions with the visual information.

Another application is a dynamic or moving poster for advertisement [8]. In this concept, graphical images are printed on both the stator and sliders to comprise a single picture. The sliders are then moved using the electrostatic actuation, causing a portion of the poster image to physically move. When stationary, the thin form factor of

*Correspondence:
Akira Okuno
aokuno@s.h.k.u-tokyo.ac.jp
[1] Graduate School of Frontier Science, The University of Tokyo, Tokyo, Japan

the actuator makes the poster appear just like an ordinary poster. Therefore, the unexpected physical motions can surprise the viewers and can create a strong advertising impact.

As such, the actuator has proven itself to be a powerful tool for human interactions. To further enhance its capabilities for human interactions, various studies have been conducted. These studies include the development of a built-in slider detection system [12] and a motion simulator to design stator electrode patterns to generate complex slider motions [13]. These studies realize controlled slider motions along complex motion paths that can enhance expression.

Another potential direction to enhance interactivity or expression is the use of proximity detection of users or viewers. If the actuator can detect an approach of a human body, it can adjust its motion based on proximity, providing users with more immersive interactive experiences.

Human motions including proximity could be easily detected by installing external sensors or cameras. However, the use of such external devices would not be preferred in some situations. For example, if a moving poster using this system is displayed in a public space, there could be various regulations, with which the use of a camera could conflict. For such reasons, as well as for simplicity, it is preferable to integrate proximity sensing into the actuator itself. Therefore, this paper discusses the method to integrate proximity sensing function into the electrostatic actuator.

Proximity sensing can be achieved through several different physical principles, including infrared [14], electric field [15], and ultrasonic [16]. Among those principles, the one using an electric field, specifically capacitive sensing, would be the most suitable choice for the integration, as the electrostatic actuator already possesses electrodes in its stator for generating electric fields around it. By utilizing the existing electrodes, integration can be achieved without compromising the actuator's simplicity. In fact, previous studies have demonstrated that capacitive sensing can be integrated with this actuator, or its variants, in a simple manner [12, 17–19], although proximity sensing has not been explored yet.

Apart from the integration, capacitive proximity sensing has been proven to be effective in a wide range of human interactions. For example, the following studies have shown a wide range of its applications: research on installing capacitive sensors in the living environment around us such as on beds [20], tables [21], and in cars [22], research focused on achieving human interaction with robots equipped with proximity sensors [23], and research aimed at estimating human body positions or postures by arranging many sensor electrodes on the floor [24] or the wall [25]. Given the extensive range of applications demonstrated in these previous studies on the capacitive method, the integration with the actuator is expected to significantly enhance the interactivity and expand the actuator's application area as a human interface.

With that in mind, the objective of this study is to propose a method of integrating capacitive proximity sensing into a charge-induction electrostatic actuator and to demonstrate a pilot interactive actuation that changes the slider motion based on the proximity of a human hand. To realize this goal, the following two technical issues will be mainly discussed. The first issue is the circuit configuration to achieve simultaneous actuation and sensing using the same electrodes. The circuit design and its influences on actuation and sensing will be discussed. The second issue is the influence of a slider on proximity sensing. A slider of the actuator has slight conductivity on its surface to allow electrostatic actuation. When such a conductive sheet is placed over the stator electrodes, the sensing electric field emitted from the electrodes might be shielded, which can affect the proximity sensing. The paper investigates the influence of such a conductive sheet on proximity sensing, using sheets with different surface resistivities. Finally, an interactive actuation that changes the velocity of the slider according to the proximity distance of a human hand will be demonstrated.

Charge-induction electrostatic actuator

The configuration of a charge-induction electrostatic actuator is shown in Fig. 1. The actuator consists of two thin sheets or plates, which are a stator and a slider. A stator is an insulating substrate, or film, with a number of parallel thin electrodes embedded with a regular pitch of several hundred micrometers, which can be fabricated by printed circuit board (PCB) manufacturing technology or by printing. A slider is a thin plastic sheet with a slightly conductive surface and has no electrode pattern. For

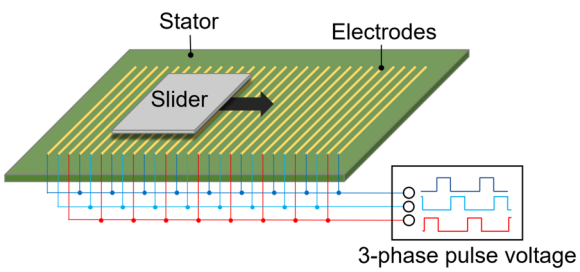

Fig. 1 Configuration of a charge-induction electrostatic actuator. This work utilizes 3-phase electrodes for the stator, to which a set of 3-phase high voltage patterns is applied

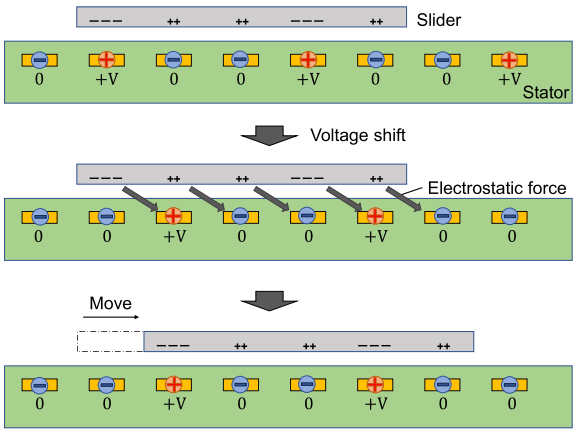

Fig. 2 Operation principle of charge-induction electrostatic actuator. In this work, two voltage levels are used to create the spatial voltage pattern. Repetition of the process moves the slider in a continuous step-wise motion

actuator operation, a slider is placed over a stator surface that will be driven by electrostatic force.

Figure 2 shows the operation of the actuator utilized in this particular work. In literature, several different voltage patterns have been proposed for operation [7, 26], and this work adopts one of the simplest patterns that consists of two voltage levels. As shown in Fig. 1, the electrodes of the stator are connected in three phases, to which high-voltage driving signals are applied. The typical driving voltage is around 1 kV.

First, as in Fig. 2, a high voltage ($+V$) is applied to one phase of the stator electrodes, and zero volts are applied to the other two phases. Then, by the electric field caused by the voltage application, surface current will flow on the slider surface that accumulates negative charges above the high voltage electrodes and positive charges above the grounded electrodes. Next, the voltage pattern is shifted by one electrode pitch, but the charges on the slider do not immediately move on the slider surface due to the low conductivity. Therefore, the electrostatic force generated on the slider charges will move the whole slider. The moving distance of the slider is approximately one electrode pitch but can vary depending on the friction or the movement of the induced charges on the slider. Repetition of this process moves the slider in a step-wise manner; the slider moves step-wise every time the voltage pattern is shifted, which is done several times to several tens of times in 1 s.

The above voltage pattern can be generated using a DC high voltage source and multiple switches. The one used in this work is shown in Fig. 3. Each phase is equipped with two switches, which are operated alternately to output either 0 V or DC high voltage (1 kV in this work) that is generated by a high voltage DC power supply. Resistors R_p are arranged to avoid large currents flowing over the relays upon switching.

Proximity sensing using actuator electrodes

This section discusses capacitive proximity sensing using a charge-induction electrostatic film actuator. First, the principle of capacitive proximity sensing and how it can be applied to the stator electrodes of the actuator are explained. Then, the concept of simultaneous actuation and proximity sensing using the same stator electrodes is discussed.

Principle of capacitance proximity sensing

Capacitive proximity sensing utilizes a phenomenon in which the electric field emitted from a sensor electrode is affected by a conductive proximity target. A human body can be regarded as an electrically conductive object, which can be detected by this sensing method. Capacitive proximity sensing can be classified into mainly two modes depending on the number of electrodes [15, 27]. These two modes are loading mode and shunt mode. Loading mode is the most common type of capacitive proximity sensing [15], as well as the simplest one as it needs only a single sensor electrode. In loading mode, the capacitance between the sensor electrode and the proximity target is measured. If this mode is applied to the electrostatic actuator, the whole stator electrodes (or the whole one-phase electrodes) could be used in a lump as a sensor electrode, as shown in Fig. 4a. In shunt mode, the sensor is equipped with two, or more, electrodes, and the capacitance between the two electrodes is measured. If used for the actuator, two phases of the 3-phase stator

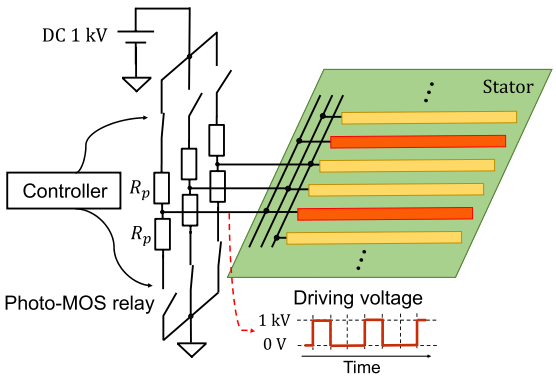

Fig. 3 Driving circuit for charge-induction electrostatic actuators

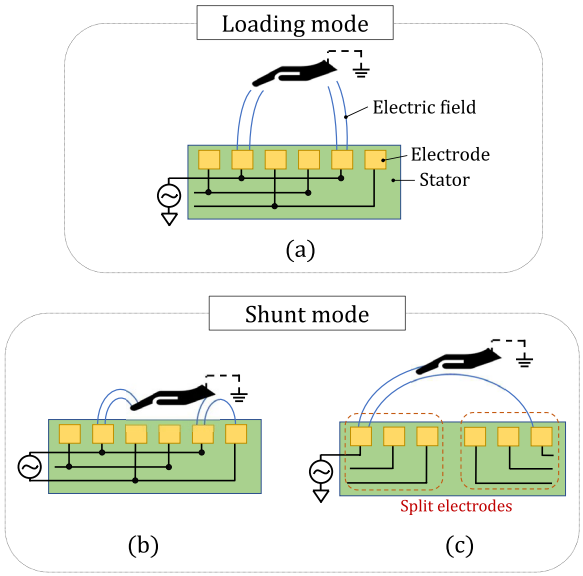

Fig. 4 Two different modes of capacitive proximity sensing. In loading mode (**a**), the capacitance between the single sensing electrode and the target will be directly measured, by assuming the target is electrically grounded. In shunt mode, the capacitance between two sensing electrodes is measured which is affected by the proximity of a target. Shunt mode can be applied to the actuator in two different ways: using two electrode phases (**b**) or splitting the actuator into two separate parts (**c**)

electrodes could be utilized as the sensing electrodes, as in Fig. 4b. If we can divide the actuator into two separate electrode sets, the two sets can be also used as the sensing electrodes in shunt mode as in Fig. 4c.

If we use a single electrode set of an actuator, which is the case of this particular paper, the two modes (a and b) will have a large difference in terms of the sensing distance. In shunt mode, the sensing distance will be roughly determined by the distance between the two sensing electrodes. Since the electrodes are aligned with several hundred micrometers in an actuator, the sensing distance in shunt mode will be considerably limited. On the other hand, in loading mode, if we use a large enough electrode, we can easily increase the capacitance change due to the proximity, which increases the measurement distance. This means that the measurement distance can be more easily extended with loading mode. Therefore, this work adopts loading mode for the integration.

Proximity sensing circuit

There are various capacitance measurement methods that can be applied to capacitive proximity sensing, which include charge measurement using a charge amplifier [28], oscillation frequency measurement [29], and impedance measurement using an AC bridge circuit [30]. In this study, impedance measurement using

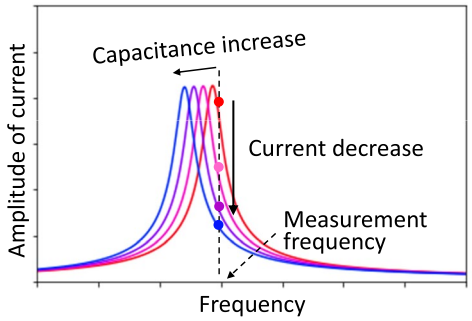

Fig. 5 Principle of capacitance measurement by a resonant circuit

a resonant circuit [31] is adopted, considering its high compatibility with the driving circuit of the actuator. The fundamental principle of the measurement using an LC resonant circuit is illustrated in Fig. 5. A constant frequency signal is applied to an LC circuit that consists of the capacitance against the target object and an inductance in the circuit. The constant frequency is set to a frequency slightly higher than the resonance frequency of the LC circuit. The resonance frequency f_{rsn} (or its angular frequency ω_{rsn}) is expressed as

$$f_{\mathrm{rsn}} = \frac{\omega_{\mathrm{rsn}}}{2\pi} = \frac{1}{2\pi}\sqrt{\frac{1}{LC}} \tag{1}$$

which shifts to the lower side when the capacitance increases. Accordingly, the amplitude of the current at the measurement frequency considerably decreases, which will be detected as proximity of a target.

The use of this measurement method has two advantages. One is that a resonant circuit can convert a slight capacitance change into a significant voltage change [32, 33] if the Q-factor of the resonance circuit is high enough. The other is its high compatibility with the use of transformers for signal superposition. Since high voltage is used for driving, it would be a natural choice to use transformers to isolate a sensing circuit from the high voltage. The transformers can be used as the inductor of the resonant circuit, which leads to a simple integrated circuit.

The proximity sensing circuit using the actuator's electrodes is shown in Fig. 6, which is to be integrated with the driving circuit. The capacitance C_0 is not necessary for proximity sensing but is arranged to decouple the sensing circuit from the driving circuit as discussed later. Two transformers are used to feed and detect a high-frequency sensing signal, as well as to provide inductance for LC resonance. Transformer L_{in} is utilized to feed the sensing signal, whereas L_{out} detects the sensing signal. In the following, the resistance of the

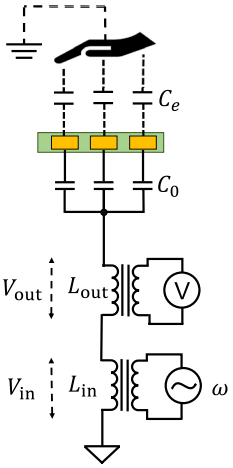

Fig. 6 Proximity sensing circuit using a stator of charge-induction electrostatic film actuator

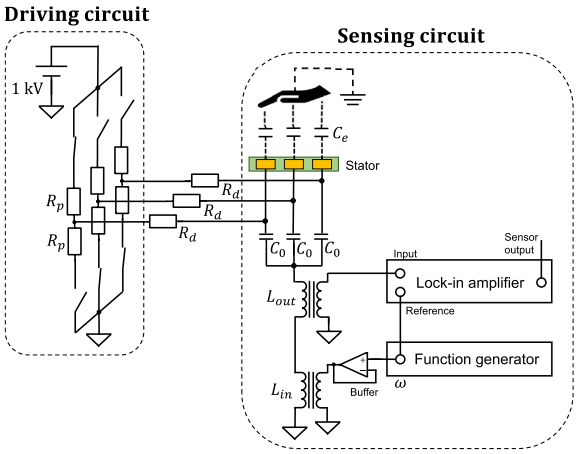

Fig. 7 Integrated circuit of driving circuit and sensing circuit

circuit, including the winding resistance of the coils, is ignored for simplicity.

Concept of simultaneous actuator driving and proximity sensing

To achieve simultaneous actuation and sensing using the same stator electrodes, two different strategies can be considered: time division and frequency division. In the time division strategy, the electrodes are connected to the sensing circuit during a short duration. For the rest of the time, the electrodes are switched to the driving circuit. This might be the simplest strategy, but the time duration that is allowed for sensing will be limited.

In the frequency division strategy, the actuation and the sensing signals coexist on the same electrode using different frequencies. Typically, the sensing signal has a high frequency, such as several tens to hundreds of kHz, whereas the actuation voltage is DC except for the moment of voltage switching. Therefore, the two signals can easily coexist, as already demonstrated in previous studies [17, 31]. As this allows proximity sensing to operate almost all the time, this strategy seems better for human interaction and thus is adopted in this work. The coexistence is realized by superposing the sensing signal onto the actuation signal using transformers. By limiting the amplitude of the sensing signal on the electrodes to tens of volts, which is sufficiently small compared to that of the actuating voltage, we can ignore the effect of the sensing signal on the actuation.

Figure 7 shows the circuit that integrates actuation and proximity sensing. The driving circuit is connected to the stator electrodes as well as the sensing circuit, through resistors R_d arranged between the two circuits. These resistors, as well as the capacitors C_0, are used to decouple the actuation and sensing.

The amplitude of the output voltage v_{out} is calculated as,

$$|v_{\text{out}}| = \frac{\omega L_{\text{out}}}{\left|\omega L_{\text{out}} - \frac{1}{\omega}\frac{1}{3C_e}\left(1 + \frac{C_e}{C_0}\right)\right|}|v_{\text{in}}| \tag{2}$$

where the input voltage is $v_{\text{in}} = \sin \omega t$ and the capacitance between one phase of the stator electrodes and the target is expressed by C_e, which is to be measured in this circuit. Since the capacitance C_0 is connected in series with the target capacitance C_e in the sensing circuit, it should be large enough compared to C_e; otherwise, the change of C_e will be almost hidden. On the other hand, for the driving circuit, C_0 is located in parallel with the actuator. Therefore, if C_0 is too large, it will affect the performance of the driving circuit by increasing the load. Considering this trade-off, C_0 was empirically selected to be of the same order as the capacitances of the actuator's electrodes, in the experiments of this work.

The resonant frequency of the sensing circuit f_{rsn} is as follows:

$$f_{\text{rsn}} = \frac{\omega_{\text{rsn}}}{2\pi} = \frac{1}{2\pi}\sqrt{\frac{1}{L_{\text{out}}}\left(\frac{1}{3C_0} + \frac{1}{3C_e}\right)} \tag{3}$$

For the sensing principle shown in Fig. 5 to work, the sensing frequency needs to be set slightly higher than this resonance frequency. The inductance L_{out} should be selected such that the sensing frequency falls within the measurable range of the apparatuses.

Possible interference

In the integrated circuit shown in Fig. 7, the two circuits are connected using decoupling resistance R_d and capacitance C_0. The function of R_d is to prevent the sensing signal from flowing into the driving circuit. If there is no resistance, a large part of the current flows into the driving circuit, which lowers the Q-factor of the resonance and decreases the sensing sensitivity. For the sensing circuit to work ideally, the resistance R_d should be infinite.

The resistance also affects the performance of the driving circuit. The sensing circuit includes capacitor C_0, as well as the capacitance between two adjacent phases although this is not indicated in the figure. These capacitances together with the resistances (R_d and R_p) delay the rising of the driving voltage. When R_d is large enough than R_p, the time constant for the voltage rise is almost proportional to R_d. A large time constant will deform the driving waveform and deteriorate the driving performance. This means a smaller R_d is better for actuation, which contradicts the requirement from the sensing circuit. To find a good compromise in this trade-off relationship, the effect of R_d on both actuation and sensing will be investigated in the following experimental section.

Experimental setup

Actuator

The stator utilized in this study was fabricated as a PCB and had an array of 552 electrodes, each measuring 255 mm long and 0.3 mm wide and aligned with a constant pitch of 0.6 mm, see Fig. 8. The stator surface was covered with a low-friction plastic film to reduce the surface friction. The 552 electrodes were connected in a 3-phase manner, with each phase comprised of 184

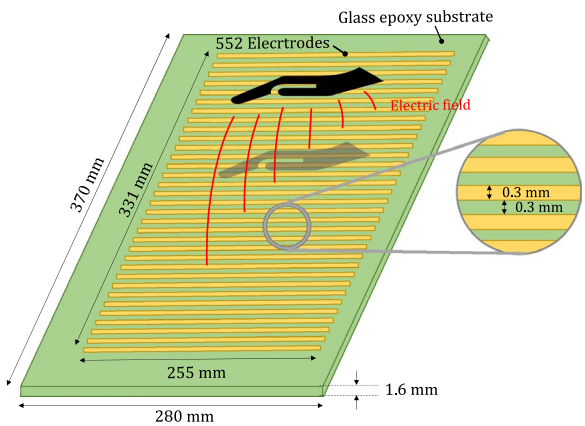

Fig. 8 Schematic figure of actuator stator and its use for loading mode capacitive proximity sensing

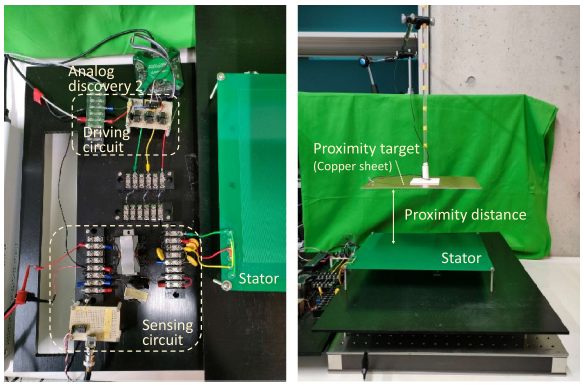

Fig. 9 Appearance of experimental setup. **a** Circuits connected to the stator electrodes. **b** Proximity method using a copper plate as a target

electrodes. In the following experiments, the stator was arranged above a horizontal metal plate, which was electrically grounded. The metal plate formed a capacitance against the actuator electrodes. Since this additional capacitance can hide the slight change of the capacitance by the proximity motion of a human body, the capacitance to the metal plate should be kept small. Therefore, to decrease the capacitance between the electrodes and the plate, the stator was placed at a height of 120 mm from the plate surface. Then, a slider, whose surface conductivity was about 4×10^{14} Ω/sq., was placed over the stator.

Circuit

To implement the integrated circuit in Fig. 7, a high voltage DC power supply (HJPM-2R7.5, Matsusada) was used to generate 1.0 kV for actuation. The high voltage was switched using Photo-MOS relays (AQV258, Panasonic) that were controlled by Analog Discovery 2 (Digilent). For the protection of the driving circuit, resistors $R_p = 100$ kΩ were used.

In the sensing part, the sensing signal was generated by a function generator (1940, NF Corporation). The output of the circuit was measured using a lock-in amplifier (LI 5650, NF Corporation) that detected the amplitude of the sensing signal obtained from the output transformer. The circuit parameters were as follows; $|v_{\text{in}}| = 0.1\ V$, $L_{\text{in}} = 7.4$ mH (turns ratio of 1:1), $L_{\text{out}} = 74$ mH (turns ratio of 0.28:1) and $C_0 = 2.2$ nF. The capacitance between two electrode phases was about 1.7 nF. The frequency of the sensing signal was chosen such that the phase of the output voltage was shifted by 20 deg from that at the resonant frequency. The frequency was adjusted in each experiment and was about 55 kHz.

The appearance of the circuit is shown in Fig. 9a. To reduce the stray capacitance formed by the cables, the sensing circuit was placed close to the stator, and the cable length was shortened. In the experiments of proximity measurement, the setup shown in Fig. 9b was utilized. As the human body can be assumed to be sufficiently conductive, a copper plate was used as the proximity target, in substitution for the human body, and its distance to the stator was changed. The copper plate had the size of 204 mm × 305 mm and was connected to the ground voltage.

Experiments

Influence on actuator driving velocity

First, the influence of resistor R_d on actuation was evaluated. As described above, larger R_d will result in a longer time constant of voltage switching. If the time constant becomes longer, the rise and fall of the pulse voltage becomes less sharp, resulting in poor driving performance.

To confirm this, two experiments were conducted. First, using different values of R_d from 0 Ω to 10 MΩ, the transient responses of the driving voltage and the slider motion were measured. The size of the slider was 100 mm × 100 mm, and a cardboard-made marker was attached to it [12] to enable the use of a laser displacement sensor (ZX1-LD70, OMRON). The slider weight including the marker was 1.6 g.

The responses are shown in Fig. 10. The voltage waveform shown in the plot was recorded by an oscilloscope. Because of the input resistance of the oscilloscope, the recorded voltage was attenuated from the actual voltage that should occur without the oscilloscope. Therefore, in the plot, the voltage was normalized to focus on the time responses. Although the time response could also be affected by the input resistance, that is ignored here. As shown in the plot, as the resistance R_d increased, the rising of the voltage slowed down. The same tendency was observed in the voltage fall. The lower plot showed the corresponding slider displacement. Larger R_d resulted in a slower response, as well as a shorter moving distance, of the slider.

Subsequently, the effect of resistance R_d on the average velocity of the slider was evaluated. The average velocity of the slider was measured with different R_d and driving frequency f_d. In each measurement, the slider was driven over the distance of 70 mm, which is the measurement range of the displacement sensor, and the average velocity was calculated.

The result is shown in Fig. 11. The upper plot indicates the average velocity and the lower plot shows the ratio of the velocity compared to the case without the sensing circuit (reference value). From the upper plot, it is confirmed that the velocity was almost proportional to the driving frequency regardless of R_d. However, the lower plot shows that there was a slight decrease in the velocity when larger R_d were utilized. With R_d being equal or less than 2.0 MΩ, the velocity was in most cases within the range of ±1% from the reference value. However, with R_d of 5.1 MΩ and 10 MΩ, the velocity ratios were lower

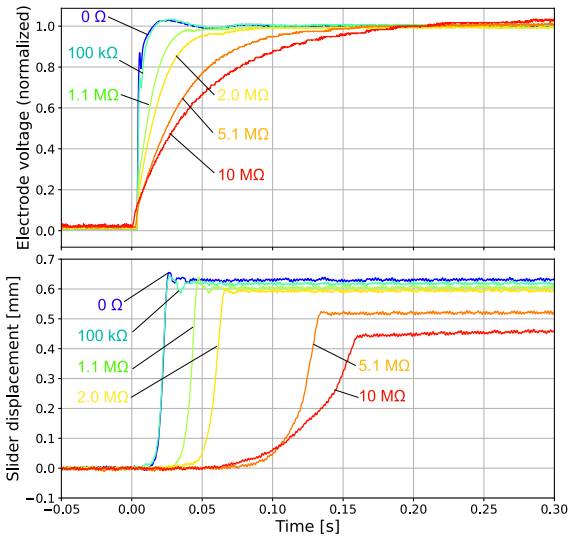

Fig. 10 Transient responses of the driving voltage and the slider displacement with different resistance R_d. The electrode voltage was measured by an oscilloscope and was affected by its input impedance

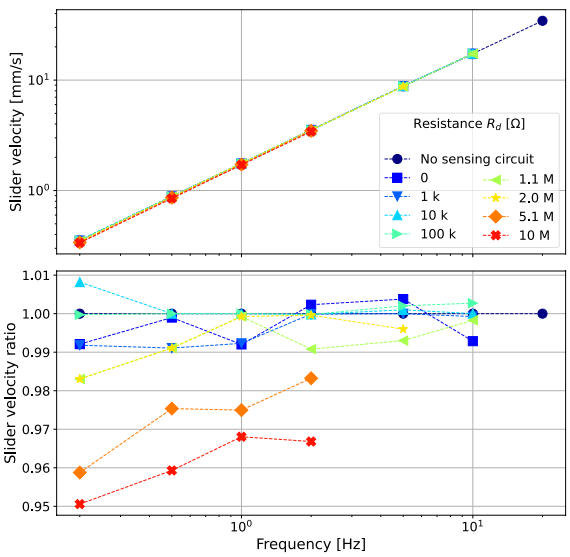

Fig. 11 Slider velocity ratio with resistance R_d compared to the case of no sensing circuit

than the reference value. This is due to the decreased step length with large R_d, as shown in Fig. 10. As these two experiments were conducted at different times, the ratio of the step lengths found in Fig. 10 does not perfectly match with the ratio of the average velocity in Fig. 11; the results can vary depending on the surface conditions, such as friction, and environmental conditions, such as humidity. However, they both show the same tendency, and the results in Fig. 10 clearly explain the reason for the decrease in the average velocity.

Moreover, the maximum frequency f_{max} usable for driving was found to decrease with R_d. While the slider could be driven with the frequency up to 20 Hz when the driving circuit alone was utilized without R_d, f_{max} was restricted to 10 Hz for R_d ranging between 0 and 10 kΩ, 5 Hz for R_d of 2.0MΩ and 2 Hz for R_d larger than 5.1 MΩ. These results matched with the results in the lower plot of Fig. 10. It was confirmed that f_{max} was closely related to the time required to complete one motion step. If we define the time to complete one motion step as t_m, the following relationship can be found: $f_{max} \approx 1/(3t_m)$. In other words, if the voltage is switched before a motion is completed, the slider cannot be actuated stably. (It should be noted that the voltage is switched 3 times within one cycle of the driving voltage waveform.) These results reveal that larger resistance R_d increases t_m, which results in a limited maximum frequency. Therefore, smaller R_d is preferred in terms of actuation.

Influence on the sensitivity of proximity sensing

Next, the influence of R_d on the sensing performance was evaluated. First, the resonance characteristics were investigated. In the proposed circuit, the proximity sensor sensitivity is determined by the Q-factor, or the sharpness, of the resonance curve because the slope of the resonance curve amplifies the capacitance change. To evaluate the relationship between the resistor R_d and the resonance curve, frequency responses were recorded with different values of R_d. The results are shown in Fig. 12. The infinite R_d means that the driving circuit was not connected. The plot clearly shows that as R_d decreases, the sharpness of the resonance curve also decreases.

Subsequently, the sensor output change due to the proximity motion was investigated. By changing the proximity distance between the stator and the copper plate, the change in sensor output before and after proximity with various R_d was measured. The result is shown in Fig. 13. It is confirmed that smaller R_d results in lower output change. Without the driving circuit, the sensor output showed an apparent difference even at distances over 40 cm. If the driving circuit was connected and resistance R_d was 10 MΩ, the sensor output change was decreased to about half of its original value. Furthermore,

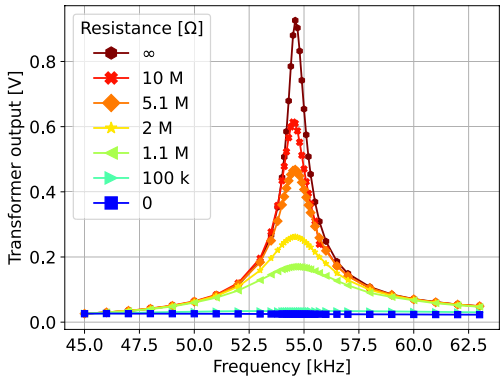

Fig. 12 Frequency responses of transformer output with different resistance R_d

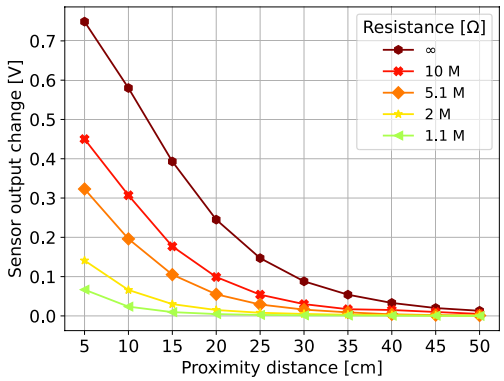

Fig. 13 Sensor output change vs proximity distance with different resistance R_d

with R_d of 1.1 MΩ, the proximity detection becomes difficult even at a distance of 30 cm. When R_d is 100 kΩ, the apparent resonance peak was not detected and the sensing could not be achieved. These results indicated that small R_d deteriorates proximity sensing performance.

To summarize this section, resistance R_d between the driving circuit and the sensing circuit should be larger in terms of sensing and smaller in terms of actuating. In the particular setup of this work, the usable range of R_d was found between 1.1 MΩ and 10 MΩ. This range would vary with the setup, but for setups with a similar scale, R_d of several MΩ might be utilized.

Evaluation of the influence of slider on proximity sensing

In a charge-induction electrostatic actuator, a slightly conductive slider exists on the actuator electrode that is also used as the sensing electrode for proximity sensing. As this location is in-between the sensing electrodes and the proximity target, the conductivity of the slider may

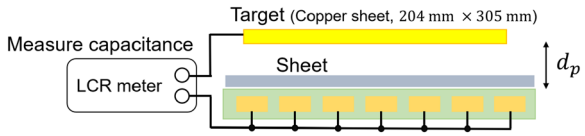

Fig. 14 Setup for measurement of capacitance between stator electrodes and a proximity target

Table 1 Sheets utilized for the measurement and their surface resistivitie

Sheet	Surface resistivity [Ω/sq.]
Actuator slider	4×10^{14}
Newspaper	7×10^{12}
Conductive sheet	7×10^{5}
Aluminum plate	<< 1

affect the proximity sensing. In this section, the influence of the sheets placed on the sensor electrode is experimentally evaluated.

Experimental setup

To investigate the influence of conductive sheets on capacitive proximity sensing, several different sheets with different surface conductivities were placed on the stator to cover all the stator surface, and the capacitance between the stator electrodes and a proximity target, which was arranged above the actuator, was measured.

The schematic diagram of the experimental setup is shown in Fig. 14. As a proximity target, a copper plate was fixed above the stator electrode like Fig. 9b. Then, the capacitance between the target and the stator electrodes, with all the three-phase electrodes connected, was measured using an LCR meter (ZM2372, NF Corporation). The capacitance was measured by varying four parameters; (1) surface resistivity of the sheet, (2) measurement frequency, (3) proximity distance between the target and the stator, and (4) electrical condition of the sheet. Table 1 shows the four sheets used in the experiments, whose surface resistances range from almost zero to 10^{14} Ω/sq. Surface resistivities shown in the table were measured by a high resistance meter (8340A, ADC Corporation). The measurement frequency was varied among 1, 10, and 100 kHz. The proximity distance was changed among 5, 10, 15, 20, and 25 cm. The two electrical conditions were applied to the sheet, which are open and grounded. In the condition of grounded, the sheet was connected to the electrical ground of the setup at one end of the sheet by a clip. In each condition, capacitance was measured 5 times and the average value was calculated.

Results and discussions

The measurement results are shown in Fig. 15. In the plot, "no sheet" represents the original condition, where no conductive sheet was placed on the stator (thick blue lines).

In (a), (c), and (e), when the sheets were in the electrically open condition, the capacitance did not change regardless of the existence of a sheet. Also, almost no frequency dependence was found. These results indicate that proximity sensing is possible even when a sheet is placed over the sensor electrodes. Even if it is a highly conductive sheet, the sensing is still possible as long as the sheet is in the electrically open condition. It was also found that the capacitance slightly increased when an aluminium plate or a conductive sheet was inserted, which has relatively higher conductivity. The cause of the increase would be that the electric potential of these sheets followed that of the sensing electrode such that they worked as a part of the sensing electrodes (which results in a slightly reduced distance against the target).

On the other hand, in (b), (d), and (f), where the sheets were electrically grounded, capacitance differed due to the sheet surface resistivity and the frequency. As for the aluminum plate, the capacitance was not detected by the LCR meter ("error" was displayed) regardless of the frequency and the proximity distance, which meant that the capacitance was too small. This suggests that the electric field from the stator electrodes was almost completely shielded by the grounded aluminum plate. In opposite to that, when the slider or the newspaper was placed, capacitance was not decreased. This is probably because the surface potential cannot be kept at the ground due to high surface resistivity, and rather follow the potential of the sensing electrodes in these lower conductive sheets. The resulting behavior became similar to that in the open condition. Finally, as for the conductive sheet with a surface resistivity of 7×10^5 Ω/sq., the capacitance was different depending on the sensing frequency. At the lowest frequency (1 kHz), the conductive sheet behaved in the same manner as the aluminum plate. At higher frequencies, however, measurable capacitance existed at a close proximity. This implies that the behavior of the conductive sheet becomes closer to that of insulating sheets at higher frequencies.

To summarize, the following can be concluded. First, when a sheet on the sensor electrode is electrically opened, proximity sensing is still possible regardless of the surface resistivity of the sheet. Second, when a sheet

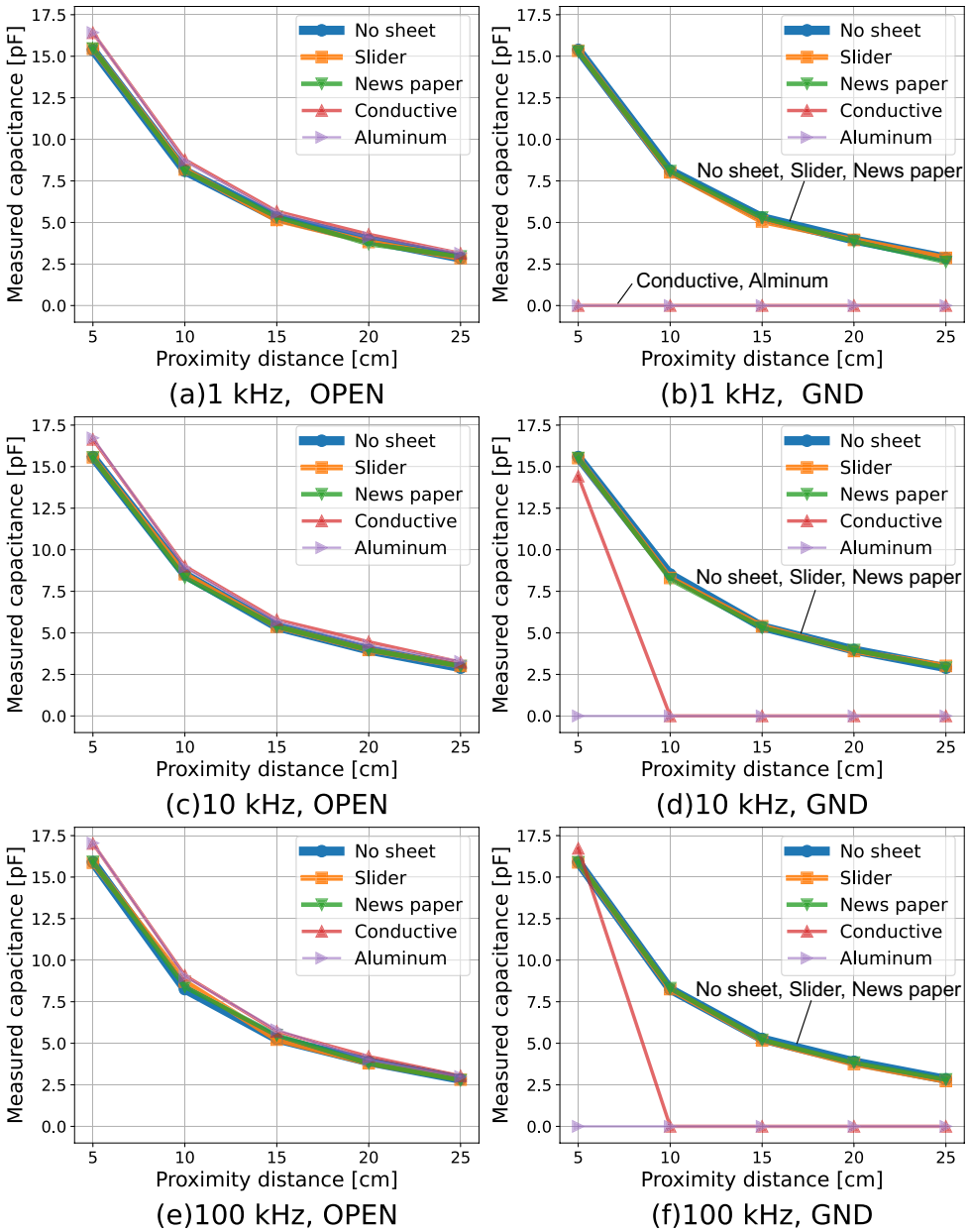

Fig. 15 Capacitance between a stator electrode and a proximity target while a sheet is arranged in-between. Capacitance = 0 means an error on the LCR meter, which indicates that capacitance is too small. In **a**, **c** and **e**, all five lines are overlapping. In **b**, **d** and **f**, blue, orange, and green lines are overlapping

is electrically grounded, a sheet with smaller surface resistivity can shield the electric field for proximity sensing, especially at lower frequencies. If, however, the surface resistivity is high enough, the sheet does not affect the proximity sensing even if it is grounded. In the experimental environment, the threshold was found around 10^5 Ω/sq.

In charge-induction electrostatic actuators, the surface resistivity of the slider is between 10^{13} and 10^{15} Ω/sq. [7], which is above the threshold. This means that the existence of the slider will not disturb the proximity sensing.

Interactive actuator operation based on the proximity distance of human hand

Using the knowledge obtained so far, an interactive actuator operation via proximity motion of the human body was carried out. In this section, the resistance R_d

was set to 5.1 MΩ, which gave much weight to the sensing range rather than the actuation performance.

In the previous sections, a copper plate was used as the proximity target, but in this section, a human hand is brought into proximity to the actuator. Therefore, at first, the relation between the hand position and the sensor output change was experimentally investigated. The proximity distance between the stator and the hand was adjusted by using a pole for height adjustment, as illustrated in Fig. 16a. The hand position was also changed horizontally. As depicted in Fig. 16b, the horizontal position was changed among three locations: the center and the edge of the stator electrodes and the half location between them. The measurement was conducted three times at each position. The change of the sensor output with and without the hand, normalized by that for the copper plate, is shown in Fig. 16c. The output change for the hand proximity was about 0.45 ~ 0.65 times that for the copper plate proximity when the horizontal position was the center. The primary factor of this capacitance decrease is considered to be the difference in the surface areas of the hand and the plate. Another difference was grounding conditions; the plate was directly connected to the electric ground by wire but the human body was not. Fig. 16c also indicates that the sensor output change becomes smaller as the hand location approaches the edge. This means that, in this system, the vertical and horizontal information interfere. Therefore, in the next experiment, the horizontal position of the hand was almost fixed to the center.

Finally, an interactive actuator driving depending on the proximity motion of a human hand was conducted. In the interactive system, the sensor output was fed to Analog Discovery 2 which controlled the actuating voltage pattern. A slider with the size of 100 mm × 100 mm was placed on the stator and its motion was controlled based on the proximity of a hand.

In this setup, the slider speed was controlled by the proximity distance. When a hand was away from the actuator, the slider was kept stationary. As the hand approached the actuator, the slider speed was gradually increased, as in Table 2. As in the table, the proximity was divided into four discrete sections such that the velocity changes could be clearly recognized in this experiment.

Figure 17 shows the time variation of the sensor output, the voltage at one phase of stator electrodes, the slider displacement, and the slider velocity. The figure indicates the velocity change of the slider when the hand is gradually brought closer to the actuator until $t = 16\,s$ and then moved away again. It was successfully confirmed that when the hand approached the actuator, the period of the driving voltage was shortened and the slider velocity increased accordingly. The proximity distance at

Table 2 Control parameters of interactive operation

Sensor output (V)	Driving frequency (Hz)
0 ~ 0.008	0.0
0.008 ~ 0.03	0.6
0.03 ~ 0.15	1.2
0.15 ~	1.8

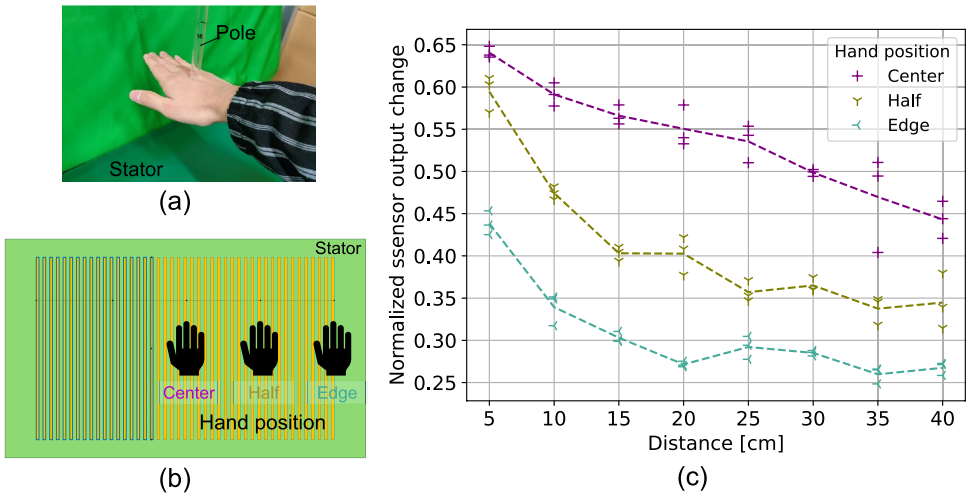

Fig. 16 Experiment to detect hand proximity. **a** height adjustment for a hand. **b** hand position in the horizontal direction. **c** The change of sensor output with and without a proximity target, normalized by that for a copper plate. The dashed lines indicate the average of the three measurements

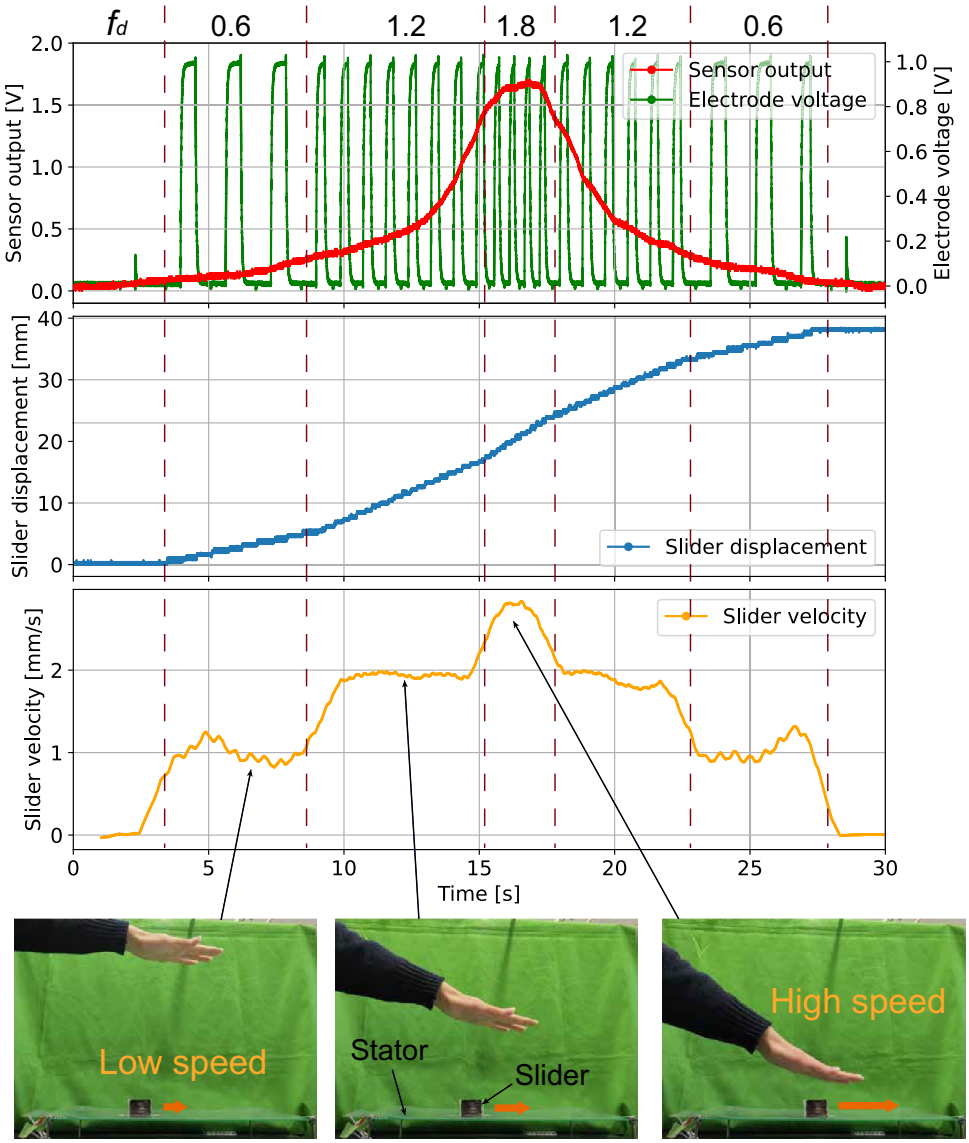

Fig. 17 Interactive actuator driving according to the proximity motion of the human hand. The red line indicates the proximity sensor output and the green line indicates the driving voltage measured on one electrode phase

which actuation initiates was longer than 300 mm. This result confirmed that proximity sensing can be integrated with the driving of the actuator without noticeable interferences.

Conclusions

This paper discusses proximity sensing on a charge-induction electrostatic actuator to realize an interactive system in which the actuator can be controlled by the proximity of a hand. The proximity sensing was realized using the same electrodes as the actuator driving. The paper proposed a circuit configuration to allow sharing of the same electrodes by sensing and driving. In the circuit, the sensing signal was superposed on the driving pulse signal using transformers. The proximity sensing circuit utilizes LC resonance between the inductance of the transformers and the capacitance caused by the proximity. The paper discussed the potential interference between the sensing and driving circuits to illustrate the trade-off relationship between the driving performance and the sensing sensitivity. In an experiment, a suitable parameter was chosen to effectively mitigate the trade-off, resulting in a driving frequency of 1.8 Hz and a sensing range of 300 mm.

In the actuator, a slightly conductive slider is placed on the stator electrodes, which work as the sensing electrodes as well. The paper investigated the impact of having a conductive sheet between the sensing electrodes and a target. The experiments confirmed that proximity sensing is not affected if a conductive sheet on the electrodes is in an electrically open condition, regardless of the conductivity of the sheet. If a conductive sheet is connected to the electric ground, its impact depends on the conductivity (or resistivity). If the resistivity is large enough, which is the case for the actuator's slider, the proximity sensing is not affected. The boundary of the resistivity was found around 10^5 Ω/sq. for sensing frequencies in the kHz order.

Finally, an interactive actuation control was demonstrated, in which the slider speed was modulated based on the distance of a hand.

In this work, a single stator board was utilized, and the sensor could not discriminate the vertical and horizontal motions of the proximity target. If multiple stator electrodes can be used, it will be possible to measure the horizontal motion of a proximity target, as well. Additionally, in the case of multiple stators, a different sensing mode (as in Fig. 4c, for example) can be utilized, which might exhibit different characteristics. Such aspects will be addressed in our future studies, to achieve unique interactions utilizing hand gestures.

Acknowledgements
One of the authors (A. O.) was supported by a scholarship from The SATOMI scholarship foundation and by JST SPRING, Grant Number JPMJSP2108.

Author contributions
A.O. and A.Y. conceived of the presented idea. A.O. conducted the analysis and experiments and prepared the draft of the manuscript. A.Y. and S.Y. supervised the project and revised the manuscript. All authors read and approved the final manuscript.

Funding
The work was partially funded by Kawaguchi Electric Works.

Availability of data and materials
The data used for analysis can be accessed by contacting the corresponding author.

Declarations

Competing interests
The slider sheet and the low-friction film utilized in the work were provided by Kawaguchi Electric Works.

Received: 27 October 2023 Accepted: 6 April 2024
Published online: 15 April 2024

References

1. Egawa S, Higuchi T (1990) Multi-layered electrostatic film actuator. In: IEEE proceedings on micro electro mechanical systems, an investigation of micro structures, sensors, actuators, machines and robots. IEEE, pp 166–171
2. Niino T, Egawa S, Higuchi T (1993) High-power and high-efficiency electrostatic actuator. In: Proceedings IEEE micro electro mechanical systems, pp 236–241. https://doi.org/10.1109/MEMSYS.1993.296916
3. Ge B, Ludois DC (2016) Dielectric liquids for enhanced field force in macro scale direct drive electrostatic actuators and rotating machinery. IEEE Trans Dielectrics Electr Insul 23(4):1924–1934
4. Ge B, Ghule AN, Ludois DC (2017) Three-dimensional printed fluid-filled electrostatic rotating machine designed with conformal mapping methods. IEEE Trans Ind Appl 53(5):4348–4359. https://doi.org/10.1109/TIA.2017.2702585
5. Schaler EW, Zohdi TI, Fearing RS (2018) Thin-film repulsive-force electrostatic actuators. Sens Actuators A Phys 270:252–261. https://doi.org/10.1016/j.sna.2017.12.054
6. Zhao N, Song Z, Li Z, Shi N, Lu F, Zhang H, Mi C, Liu W (2019) Development of a dielectric-gas-based single-phase electrostatic motor. IEEE Trans Ind Appl 55(3):2592–2600. https://doi.org/10.1109/TIA.2019.2895194
7. Egawa S, Niino T, Higuchi T (1991) Film actuators: planar, electrostatic surface-drive actuators. In: Proceedings of the IEEE micro electro mechanical systems. IEEE, pp 9–14
8. Yamamoto A (2019) Integrated presentation of physical motions and visual information utilizing electrostatic force. J Jpn Soc Appl Electromagn Mech 27(4):407–411
9. Amano K, Yamamoto A (2011) An interaction on a flat panel display using a planar 1-dof electrostatic actuator. In: Proceedings of the ACM international conference on interactive tabletops and surfaces, pp 258–259
10. Amano K, Yamamoto A (2012) Tangible interactions on a flat panel display using actuated paper sheets. In: Proceedings of the 2012 ACM international conference on interactive tabletops and surfaces, pp 351–354
11. Yamashita N, Amano K, Yamamoto A (2014) Interaction with real objects and visual images on a flat panel display using three-dof transparent electrostatic induction actuators. In: Proceedings of the 2014 ACHI international conference on advances in computer-human interactions. Citeseer, pp 294–299
12. Kojima M, Yoshimoto S, Yamamoto A (2023) Slider sheet detection in charge-induction electrostatic film actuators. Sensors 23(3):1529
13. Mizutani R, Yoshimoto S, Yamamoto A, Miura S, Sakai T, Horikane S (2020): Simulation of planar slider motion on a charge-induction electrostatic actuator. In: IECON 2020 The 46th annual conference of the IEEE industrial electronics society. IEEE. pp 730–735
14. Yun J, Lee S-S (2014) Human movement detection and idenification using pyroelectric infrared sensors. Sensors 14(5):8057–8081
15. Grosse-Puppendahl T, Holz C, Cohn G, Wimmer R, Bechtold O, Hodges S, Reynolds MS, Smith JR (2017) Finding common ground: a survey of capacitive sensing in human-computer interaction. In: Proceedings of the 2017 CHI conference on human factors in computing systems, pp 3293–3315
16. Huang Y, Newman K (2012) Improve quality of care with remote activity and fall detection using ultrasonic sensors. In: 2012 annual international conference of the IEEE engineering in medicine and biology society. IEEE, pp 5854–5857
17. Nishijima T, Yamamoto A, Yasui H, Higuchi T (2006) A built-in displacement sensor for an electrostatic film motor. Meas Sci Technol 17(10):2676. https://doi.org/10.1088/0957-0233/17/10/020
18. Zhang G, Yamamoto A (2021) Position estimation of synchronous electrostatic film motors under pulse-voltage operation by using driving currents. Sens Actuators A Phys 332:113154. https://doi.org/10.1016/j.sna.2021.113154
19. Zhang G, Yamamoto A (2023) Position self-sensing for electrostatic motors under amplitude-modulated ac operation. IEEE Trans Ind Electr. https://doi.org/10.1109/TIE.2023.3306415
20. Rus S, Grosse-Puppendahl T, Kuijper A (2017) Evaluating the recognition of bed postures using mutual capacitance sensing. J Ambient Intell Smart Environ 9(1):113–127
21. Wimmer R, Kranz M, Boring S, Schmidt A (2007) Captable and capshelf-unobtrusive activity recognition using networked capacitive sensors. In: 2007 fourth international conference on networked sensing systems. IEEE, pp 85–88
22. Frank S, Kuijper A (2019) Robust driver foot tracking and foot gesture recognition using capacitive proximity sensing. J Ambient Intell Smart Environ 11(3):221–235

23. Navarro SE, Mühlbacher-Karrer S, Alagi H, Zangl H, Koyama K, Hein B, Duriez C, Smith JR (2021) Proximity perception in human-centered robotics: a survey on sensing systems and applications. IEEE Trans Robot 38(3):1599–1620
24. Faulkner N, Parr B, Alam F, Legg M, Demidenko S (2020) Caploc: capacitive sensing floor for device-free localization and fall detection. IEEE Access 8:187353–187364
25. Zhang Y, Yang C, Hudson SE, Harrison C, Sample A (2018) Wall++ room-scale interactive and context-aware sensing. In: Proceedings of the 2018 Chi conference on human factors in computing systems, pp 1–15
26. Yamamoto A, Tsuruta S, Higuchi T (2010) Planar 3-dof paper sheet manipulation using electrostatic induction. In: 2010 IEEE international symposium on industrial electronics, pp 493–498. https://doi.org/10.1109/ISIE.2010.5637849
27. Smith JR (1999) Electric field imaging. PhD thesis, Massachusetts Institute of Technology
28. Novak JL, Feddema IT (1992) A capacitance-based proximity sensor for whole arm obstacle avoidance. In: Proceedings 1992 IEEE international conference on robotics and automation, pp 1307–13142. https://doi.org/10.1109/ROBOT.1992.220068
29. Benniu Z, Junqian Z, Kaihong Z, Zhixiang Z (2007) A non-contact proximity sensor with low frequency electromagnetic field. Sens Actuators A: Phys 135(1):162–168
30. Iqbal J, Lazarescu MT, Tariq OB, Lavagno L (2017) Long range, high sensitivity, low noise capacitive sensor for tagless indoor human localization. In: 2017 7th IEEE international workshop on advances in sensors and interfaces (IWASI). IEEE, pp 189–194
31. Yamamoto A, Suzuki J (2014) Position estimation in singly-fed electrostatic actuation systems by superposing sensing signals. Appl Mech Mater 541:1487–1491
32. Miller G, Wagner E, Sleator T (1990) Resonant phase shift technique for the measurement of small changes in grounded capacitors. Rev Sci Instr 61(4):1267–1272
33. Li H, Xiang D, Han X, Zhong X, Yang X (2019) High-accuracy capacitance monitoring of DC-link capacitor in VSI systems by LC resonance. IEEE Trans Power Electron 34(12):12200–12211

Publisher's Note